In Vivo Expression of mRNA for the Ca^{++}-binding Protein SPARC (Osteonectin) Revealed by In Situ Hybridization

Peter W. H. Holland, Sarah J. Harper, John H. McVey, and Brigid L. M. Hogan

Laboratory of Molecular Embryology, National Institute for Medical Research, London NW7 1AA, England

Abstract. In situ hybridization is used to survey the tissue-specific and developmental expression of the cloned mouse gene *Sparc*, coding for a protein homologous to the bovine Ca^{++}-binding protein, osteonectin. High levels of SPARC RNA are found in osteoblasts and odontoblasts. In addition, high grain counts are associated with a variety of other cell types in the embryo and newborn mouse, including parietal endoderm, deciduum, whisker follicles (connective tissue sheath), peripheral nerve trunk, skin (dermis), and stomach (submucosa). Spatially restricted but high levels of SPARC mRNA are also seen in the adult adrenal glands, testis, and ovary. This pattern of differential gene expression demands a reassessment of the function originally proposed for osteonectin, and predicts a much wider role for the protein in a variety of biological processes.

SPARC is a glycoprotein with an M_r of 43,000 initially cloned as a major secreted product of parietal endoderm cells that are specialized for the synthesis of a thick basement membrane (Reichert's membrane) surrounding the mouse embryo (Mason et al., 1986*a*, *b*). These studies also provided evidence that SPARC is identical to a glycoprotein (43K) synthesized in culture by bovine endothelial cells and by fibroblasts from fetal bovine dermis and nuchal ligament (Sage et al., 1984; Sage, 1985). Recently, it has also become apparent that SPARC is identical to the calcium-binding protein osteonectin, originally isolated from fetal bone and dentine (Termine et al., 1981*a*, *b*). The first 10 NH_2-terminal amino acids of the bovine 43K protein match the corresponding residues of bovine osteonectin (Mason et al., 1986*a*; Romberg et al., 1985; Young et al., 1986). When this comparison is extended to the complete amino acid sequences predicted from the cDNAs of mouse SPARC and bovine osteonectin (Bolander, M. E., and J. D. Termine, National Institute of Dental Research, Bethesda, MD, personal communication), 92% sequence identity is observed. In addition, both bovine osteonectin and mouse SPARC are coded for by single genes with similar exon/intron organization (Mason et al., 1986*b*; Young et al., 1986; J. H. McVey, unpublished results), and are phosphorylated (Termine et al., 1981; Romberg et al., 1985; Engel, J., W. Taylor, M. Paulsson, H. Sage, and B. L. M. Hogan, manuscript submitted for publication) and down-regulated in transformed cells (Mason et al., 1986*b*; Young et al., 1986). Osteonectin binds calcium with high affinity (K_d ~3 × 10^{-7} M kD) and delays hydroxyapatite-seeded crystal growth by 50% at a concentration of ~0.2 μM (Romberg et al., 1985). It is therefore of significance that two domains of mouse SPARC have been identified as potential sites for Ca^{++} binding (Engel, J., W. Taylor, M. Paulsson, H. Sage, and B. L. M. Hogan, manuscript submitted for publication). These are the NH_2-terminal glutamic acid–rich domain and residues 268–289, which clearly fulfill the requirements of an EF-hand Ca^{++}-binding domain as found in intracellular Ca^{++}-binding proteins such as calmodulin, troponin C, parvalbumin, vitamin D–dependent intestinal Ca^{++}-binding protein (ICaBP), and the extracellular protein, fibrinogen (Kretsinger, 1979; Szebenyi and Moffat, 1986; Dang et al., 1985).

Early studies on bovine osteonectin showed that the protein could be extracted in large amounts from fetal bone and dentine, and the ability of the protein to bind both Ca^{++} and type I collagen led to the suggestion that it promotes mineralization by initiating the deposition of hydroxyapatite on the surface of collagen fibrils (Termine et al., 1981*a*, *b*). This hypothesis was supported by the immunocytochemical localization of osteonectin in the matrix of mineralizing fetal bovine and porcine bone and dentine (Termine et al., 1981*b*; Tung et al., 1985). However, both the very high degree of sequence identity between mouse SPARC and bovine osteonectin and reports that osteonectin protein and/or RNA can be detected in noncalcified tissues such as porcine periodontal ligament, tooth pulp (Wasi et al., 1984; Tung et al., 1985), and rat tendon (Young et al., 1986), argue against a specific role for osteonectin limited to the initiation of mineralization.

Clearly, an important step towards understanding the biological significance of SPARC/osteonectin is to have a precise picture of the different cell types in which the gene is expressed at high levels, in embryonic, neonatal, and adult tissues. Studies using antibody probes are complicated by the possibility that SPARC may bind to an M_r 70,000 protein

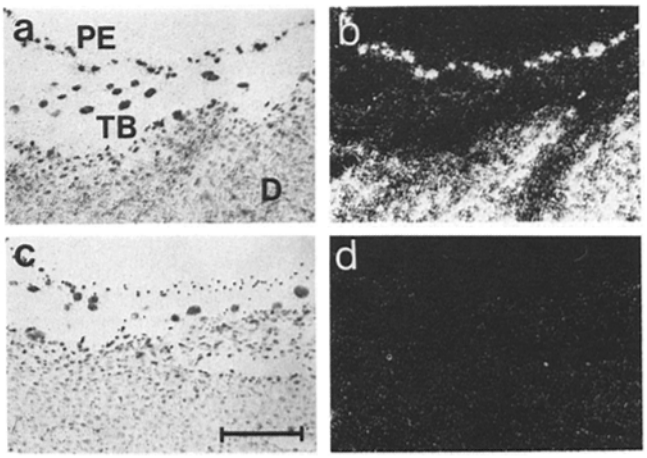

Figure 1. SPARC RNA distribution in the 8.5-d embryo. (*a*) Autoradiograph of section of materno-fetal junction showing parietal endoderm cells (*PE*) on Reichert's membrane, trophoblast giant cells (*TB*), and maternal decidual cells (*D*). Processed for in situ hybridization with − strand probe and photographed under bright field illumination. (*b*) Same field as *a* photographed under dark ground illumination. (*c* and *d*) Corresponding sections through another embryo processed with + strand probe. Slides were exposed to emulsion for 2 d. Bar, 200 μm.

and become associated with cells that do not make the protein themselves (Sage, 1986). Northern analysis of RNA isolated from dissected tissues has provided some information about patterns of expression in vivo (Mason et al., 1986*b*), but does not take into account the variety of cell types within one organ. We have therefore used the powerful technique of in situ hybridization to localize SPARC mRNA within sections of mouse tissues, using radioactively labeled single-stranded RNA probes. The pattern of gene expression observed throws new light on the function of the protein, suggesting that it has a much wider biological role than previously realized.

Materials and Methods

Preparation of Tissue Sections

All mice were of the CBA inbred strain. Noon of the day of vaginal plug is 0.5 d postcoitum. Fixation conditions were essentially as described by Brulet et al. (1985). Embryos and adult organs were fixed in 4% paraformaldehyde in PBS for 20 h at 4°C, followed by incubation in 0.5 M sucrose in PBS for 24 h. Specimens were mounted in Tissue-Tek OCT (Miles Scientific, Naperville, IL) and frozen in liquid nitrogen. Mice designated newborn were killed by etherization a few hours after birth and frozen, without prior fixation, in Tissue-Tek OCT. Blocks were stored at −70°C for up to 6 mo with no significant decrease in hybridization signal.

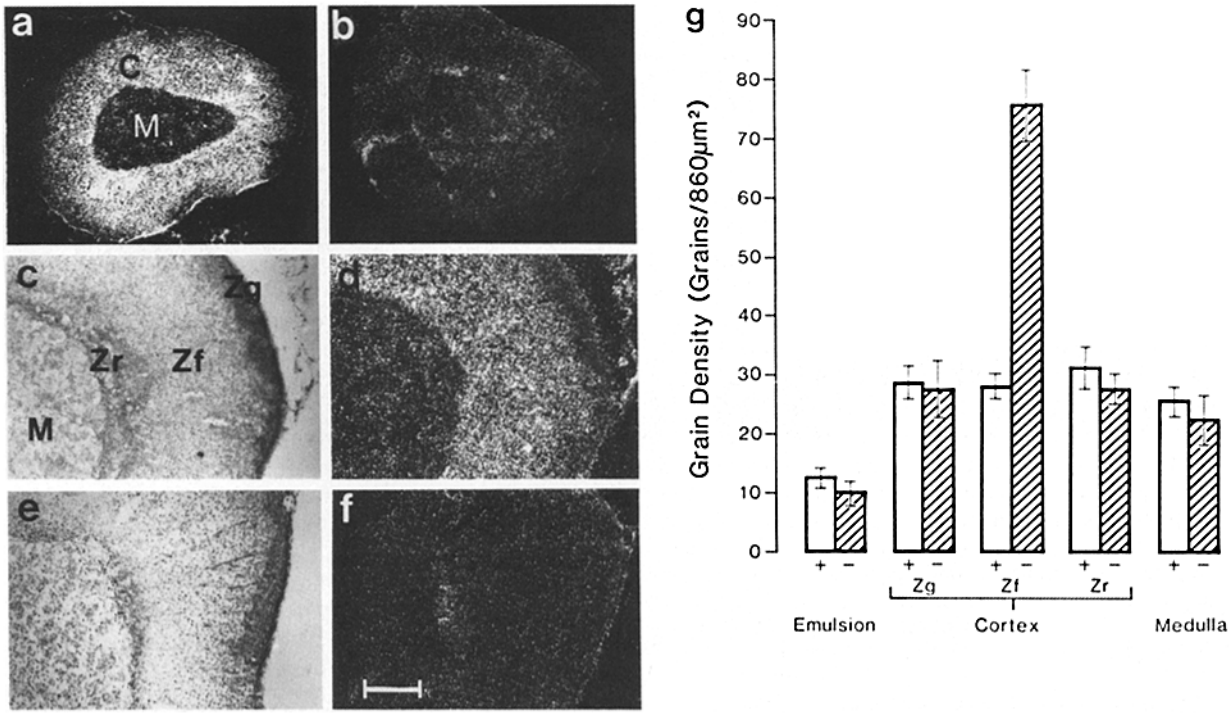

Figure 2. SPARC RNA distribution in the adult adrenal gland. (*a*) Autoradiograph of section processed for in situ hybridization with − strand probe photographed with dark ground illumination. Note higher density of silver grains over the cortex (*C*) compared with the medulla (*M*). (*b*) As in *a* except that + strand probe was used on another section of the same adrenal gland. (*c*) Detail of section shown in *a* photographed under bright field illumination. Note the medulla (*M*), zona reticularis (*Zr*), zona fasciculata (*Zf*), and zona glomerulosa (*Zg*). (*d*) Same field as in *c* photographed under dark ground illumination. Highest density of silver grains is over the zona fasciculata. (*e*) Detail of section shown in *b*, photographed under bright field illumination. (*f*) Same field as in *e* photographed under dark field illumination. All slides were exposed to emulsion for 1 day. Bar: (*a* and *b*) 400 μm; (*c–f*) 200 μm. (*g*) Graph showing quantitation of silver grains over different regions of the adrenal gland. Grain densities were calculated as described in Materials and Methods using enlargements of photomicrographs *c* and *d* for the − strand probe (*hatched bars*) and *e* and *f* for the + strand probe.

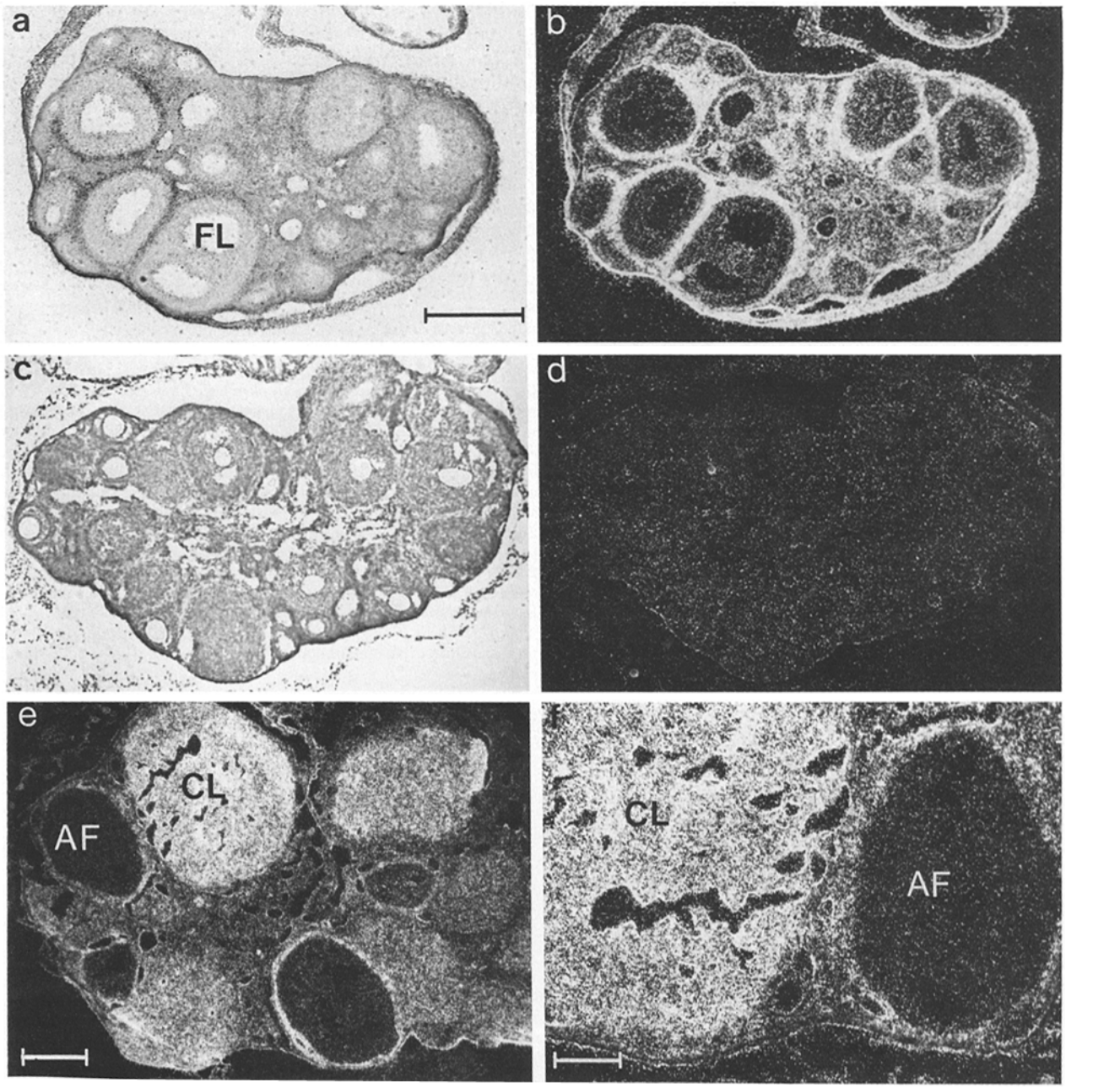

Figure 3. SPARC RNA distribution in the immature and adult ovary. (*a*) Autoradiograph of a section of an ovary from a 2-wk-old (immature) female processed for in situ hybridization with − strand probe. Photographed under bright field illumination. (*b*) The same section photographed under dark ground illumination. High densities of silver grains are seen in the thecal layer surrounding the developing follicles (*FL*). (*c* and *d*) Autoradiograph of another section through the same ovary processed for in situ hybridization with the + strand probe. Bright field (*c*) and dark ground illumination (*d*). Slides were exposed to emulsion for 6 d. (*e*) Autoradiograph of a section through an ovary from a pregnant female processed for in situ hybridization with − strand probe. High grain density is present in the thecal layer of an antral follicle (*AF*) and throughout the corpus luteum (*CL*). Dark ground illumination. (*f*) Detail of *e*. Slides exposed to emulsion for 5 d. Bars: (*a–d*) 300 μm; (*e*) 200 μm; (*f*) 100 μm.

Sections (7–10 μm) were cut on a cryostat (Slee International Inc., Tiverton, RI) at −20°C, collected on polylysine-coated slides, rapidly dried on a hotplate at 50°C for 1–3 min, and air-dried for 1–2 h at room temperature. Sections were postfixed in 4% paraformaldehyde in PBS (20 min, room temperature), rinsed in PBS (three times for 5 min at room temperature), and dehydrated. After air drying, slides were stored desiccated at −20°C for up to 6 wk.

Probe Preparation

The template used for probe synthesis (pC33.1) is a 1.1-kb genomic clone containing the extreme 3′ exon (nucleotides 970–1947, Mason et al., 1986*a*) of the SPARC gene plus 160 bp of intronic sequence, subcloned into pGEM1 (Promega Biotec, Madison, WI). ^{35}S-labeled single-stranded RNA probes (specific activity 2 × 10^9 cpm/μg) were synthesized using [α-^{35}S]UTP (New England Nuclear, Boston, MA) in SP6 and T7 RNA polymerase transcription reactions. Transcription conditions for both enzymes were as described by Melton et al. (1984) with modifications suggested by the supplier (Promega Biotec). The antisense (−) strand (i.e., complementary to SPARC mRNA) was synthesized using SP6 RNA polymerase after linearizing the template DNA with Eco RI. The sense (+) strand was synthesized using T7 RNA polymerase after linearization with Hind III, and was used for con-

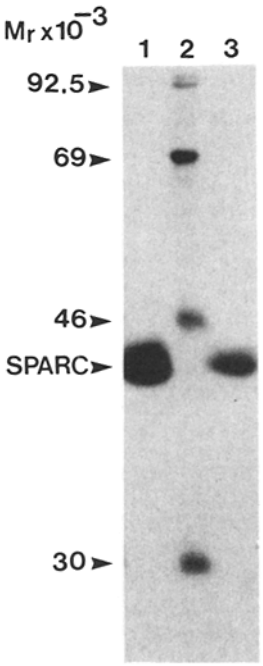

Figure 4. Synthesis and secretion of SPARC by ovarian follicle (granulosa) and PYS cells in culture. Follicle cells released from the ovaries of hormone-primed immature mice (see Materials and Methods) were cultured for 3 d before labeling for 16 h with [^{35}S]methionine. Cultures of PYS cells were labeled under the same conditions. Aliquots of medium containing equal amounts of trichloroacetic acid–precipitable radioactivity were used for recovery of SPARC by immunoprecipitation with antipeptide serum and protein A Sepharose. (Lane *1*) SPARC immunoprecipitated from the medium of PYS cells; (lane *2*) ^{14}C-labeled marker proteins; (lane *3*) SPARC immunoprecipitated from the medium of granulosa cells. Densitometer scanning of lanes *1* and *3* showed that granulosa cells synthesize and secrete ~40% the amount of SPARC that PYS cells do.

trol hybridizations. Probe size was reduced to an average size of 100 bases by limited alkaline hydrolysis (Cox et al., 1984) and was checked by formaldehyde-agarose gel electrophoresis (Maniatis et al., 1982). Probes were stored at ~0.25 ng/μl in 50% formamide, 10 mM dithiothreitol (DTT), at −20°C.

In situ Hybridization

Sections were rehydrated and prepared for hybridization essentially as described by Hafen et al. (1983), with modifications suggested by Ingham et al. (1985). Hybridization conditions were as described (Ingham et al., 1985; Hogan et al., 1986) except that probes were used at a final concentration of 0.06 ng/μl and poly(A)$^+$ was also included at 0.5 μg/μl. After overnight hybridization at 50°C, coverslips were removed by immersing slides in 50% formamide, 0.3 M NaCl, 10 mM $NaPO_4$, pH 6.8, 10 mM Tris·HCl, 5 mM EDTA, 1× Denhardt's (0.02% wt/vol Ficoll 400, 0.02% wt/vol polyvinylpyrrolidone, 0.02% wt/vol BSA fraction V), 10 mM DTT at 50°C for 10–30 min. Slides were then washed in fresh buffer at 50°C for 2–4 h with gentle stirring, rinsed in 0.5 M NaCl, 10 mM Tris·HCl, pH 7.6, 1 mM EDTA (NTE) for 15 min at 37°C, treated with 20 μg/ml RNase A (Sigma Chemical Co., St. Louis, MO) in NTE for 30 min at 37°C, and washed in fresh NTE for 30 min at 37°C. The slides were subsequently washed in 2× SSC (30 min at 45°C) followed by 1× SSC (30 min at 45°C) with gentle stirring (Cox et al., 1984). After dehydration, slides were dipped in emulsion (K5, Ilford, Knutsford, Chesire, England), diluted 1:1 with 2% glycerol in distilled H_2O, placed on a cooled metal plate for 15 min, and dried for 2 h at room temperature and humidity, followed by 6–12 h at room temperature in the presence of desiccant (Rogers, 1979). Slides were exposed at 4°C for 1–5 d, developed in D19 developer (2 min at 20°C), stopped in 1% acetic acid (1 min at 20°C), fixed in 30% sodium thiosulphate (5 min at 20°C), and rinsed in distilled H_2O (two times for 15 min at 20°C). Sections were stained in toluidine blue (0.02% for 30–90 s), dehydrated, and mounted using Permount (Fisher Scientific Co., Pittsburgh, PA). Control samples for positive and negative chemography were treated exactly as above, except that the probe was omitted from the hybridization. Control slides for negative chemography were fogged by brief exposure to light after air drying before exposure. Photographs were taken under bright field and dark ground illumination using a Zeiss Photomicroscope III, Kodak Technical Pan 24175 film, and equal exposure times for sections hybridized with + or − strand probes.

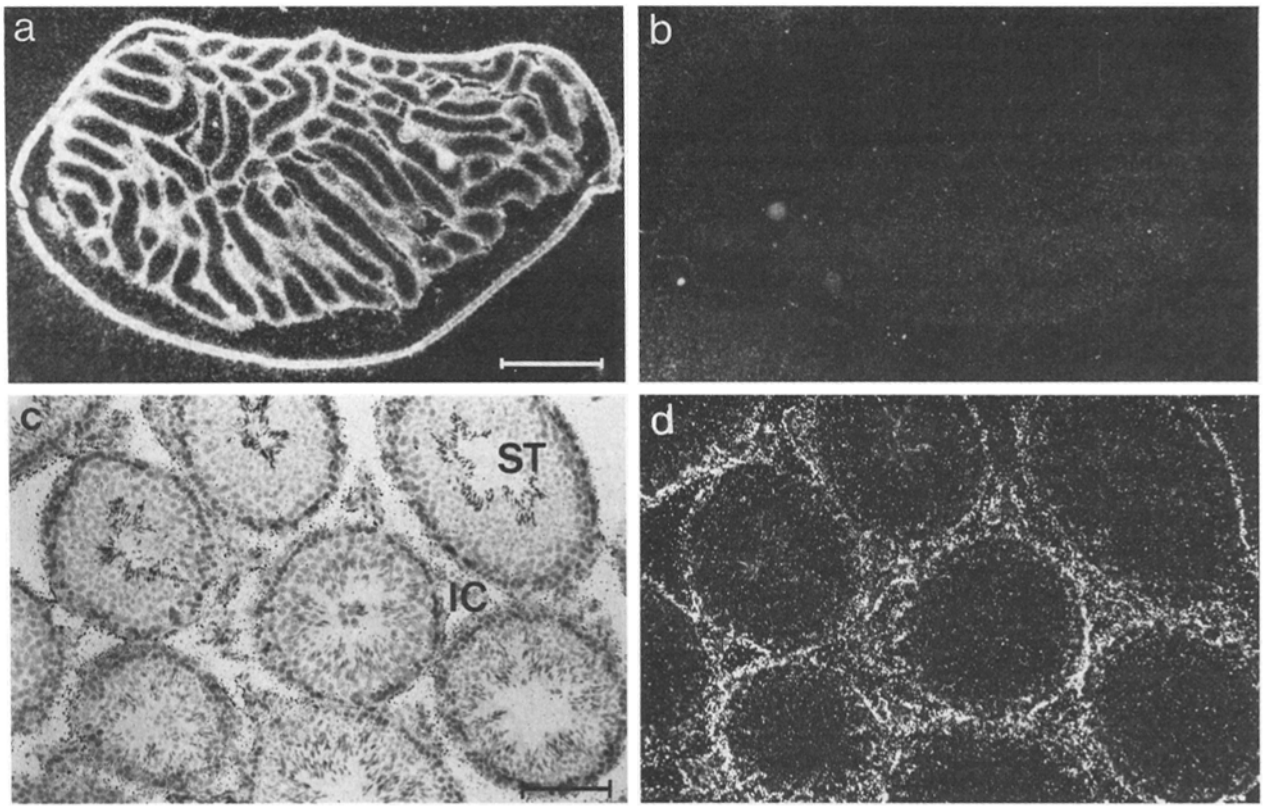

Figure 5. SPARC RNA distribution in the immature and adult testes. (*a*) Autoradiograph of a section of a testis from a 2-wk-old (immature) male processed for in situ hybridization with − strand probe. Grain density is highest in the interstitial cells between the seminiferous tubules (*ST*). Dark ground illumination. (*b*) Autoradiograph of a control section from another testis processed for in situ hybridization with + strand probe. Both slides were exposed to emulsion for 6 d. (*c*) Autoradiograph of a section from a mature adult testis processed for in situ hybridization with − strand probe. Bright field illumination. (*d*) Same field as (*c*) photographed under dark ground illumination. *IC*, interstitial cells. Exposure, 1 d. Bars: (*a* and *b*) 500 μm; (*c* and *d*) 100 μm.

Table I. Relative Levels of SPARC RNA in Some Adult and Embryonic Mouse Tissues*

High	Low	Negative
8.5-d Embryo		
Parietal endoderm	Visceral endoderm	Neurectoderm
Decidual cells of endometrium	Trophoblast	Paraxial mesoderm
Heart		
Adult mouse		
Female adrenal gland		
Zona fasciculata		Zona reticularis
		Zona glomerulosa
		Medulla
Ovary		
Thecal cells		Preovulatory follicle cells
Corpus luteum, including granulosa cells		Oocytes
Testis		
Interstitial cells, including Leydig cells		Spermatogonia
Capsule		Sertoli cells
Newborn mouse		
Periosteal cells of membrane and endochondrial bone	Lung	Most neuronal cells of the brain
	Cartilage	
	Heart	Liver
Odontoblasts	Ameloblasts	Stomach, secretory layer
Stomach, submucosa		
Thyroid, interstitial stroma		Skin, epidermis and most layers of hair follicle
Skin, dermis and connective tissue sheath of whisker follicles		
Peripheral nerve trunk (e.g., infraorbital)		

* Qualitative comparisons are made only between different cell types on the same section relative to similar sections treated with + strand probes at the same time and under the same conditions.

Quantitation of Hybridization

Four morphologically distinct regions of the adrenal gland were identified under bright field illumination (Fig. 2, *c* and *d*), and grain densities over each region (plus over emulsion only) were calculated from visual grain counts off dark ground photographs (Fig. 2, *e* and *f*). Grain number was counted in 20 equally sized areas (original size ~860 μm^2) per region for both probes (+ and −); results are presented as mean grain number per area ± two standard errors of the mean.

Metabolic Labeling and Immunoprecipitation

Homogeneous cultures of granulosa cells were established as described (Hogan et al., 1986). Immature CBA mice (12.5–14.5 gm) were injected intraperitoneally with 5 IU follicle-stimulating hormone and 48 h later with 5 IU human chorionic gonadotropin. 9 h after the last injection the ovaries were removed and clumps of follicle cells were released into Dulbecco's modified Eagle's medium plus 10% fetal bovine serum by puncturing individual follicles with a 26-gauge needle (four ovaries/35-mm tissue culture dish). After a 3-d culture the cells were labeled for 16 h with 50 μCi [^{35}S]methionine and SPARC immunoprecipitated from the culture medium with rabbit anti-SPARC peptide serum and protein A Sepharose as described (Mason et al., 1986*a*). Cultures of the mouse parietal endoderm cell line, PYS, were labeled in parallel. Samples were analyzed by fluorography after SDS-PAGE under reducing conditions as described (Mason et al., 1986*a*). ^{14}C-labeled marker proteins are myosin heavy chain (M_r 212,000), phosphorylase b (M_r 100,000 and 92,500), bovine serum albumin (M_r 69,000), ovalbumin (M_r 43,000), and lysozyme (M_r 30,000).

Results

Distribution of SPARC RNA in the 8.5-d Mouse Embryo

SPARC was first identified as a major secreted product of mouse embryo parietal endoderm cells that are actively synthesizing Reichert's basement membrane (Mason et al., 1986*a*). As expected, these cells hybridize strongly with − strand probe (Fig. 1b), while the specificity of the reaction is shown by the absence of hybridization with + strand probe. Trophoblast giant cells contain relatively little SPARC RNA, but higher levels are seen throughout the deciduum (Fig. 1, *a–d*). In the embryo itself, specific hybridization is seen in the area of the developing heart, but is absent from the neurectoderm and paraxial mesoderm (data not shown).

Distribution of SPARC RNA in Organs of Adult and Immature Mice

Earlier studies had shown by Northern analysis that SPARC mRNA is present at high levels in some adult tissues (e.g., adrenal gland, testis, ovary, and lung) but low in others (e.g., liver and brain) (Mason et al., 1986*b*). The distribution of RNA between the different cell types in three of the positive organs was therefore examined in detail (Figs. 2, 3, and 5). In all cases tissues were considered positive for SPARC RNA if they gave higher grain counts with − strand than with + strand probes.

Adrenal Gland. Hybridization of − strand SPARC probe to sections of adult adrenal gland reveals a distinct heterogeneity in RNA distribution, with much higher levels in the cortex (which is specialized for steroid synthesis) than in the medulla (the site of catecholamine synthesis by chromaffin cells) (Fig. 2, *a–f*). Quantitative analysis of the silver grains over the different regions of the cortex of adrenals from female mice (as described in Materials and Methods) suggests that SPARC expression is confined to the zona fasciculata (primarily concerned with glucocorticoid secretion), and is much lower in or absent from the zona glomerulosa (aldosterone secretion), and the zona reticularis (which is generally thought to be involved in androgen synthesis) (Fig. 2 *e*). Within the zona fasciculata, silver grains detecting the presence of SPARC RNA appear to be homogeneously distributed (Fig. 2 *d*), and are not obviously confined to a particular subpopulation of cells, e.g., the endothelium of the blood capillaries.

Ovary. In ovaries from 2-wk-old immature females, highest levels of SPARC RNA are seen in the thecal cells around the developing follicles, while levels in the follicle cells and oocytes are low (Fig. 3, *a* and *b*). With the technique used here it is not possible to distinguish between the different cell types in the thecal layer (steroid-producing cells, fibroblasts, endothelial cells of the capillary plexus), but the overall grain distribution is not consistent with expression in blood vessels alone. In ovaries from pregnant females the thecal expression is maintained, but, in addition, high levels of specific hybridization are seen throughout the corpora lutea (Fig. 3, *e* and *f*). This distribution suggests that both the steroid-secreting granulosa cells and the endothelial cells of the capillary plexus (which invades the follicle after ovulation) synthesize SPARC in large amounts. Evidence for synthesis by granulosa cells was obtained by immunoprecipitation of labeled SPARC protein from the medium of these

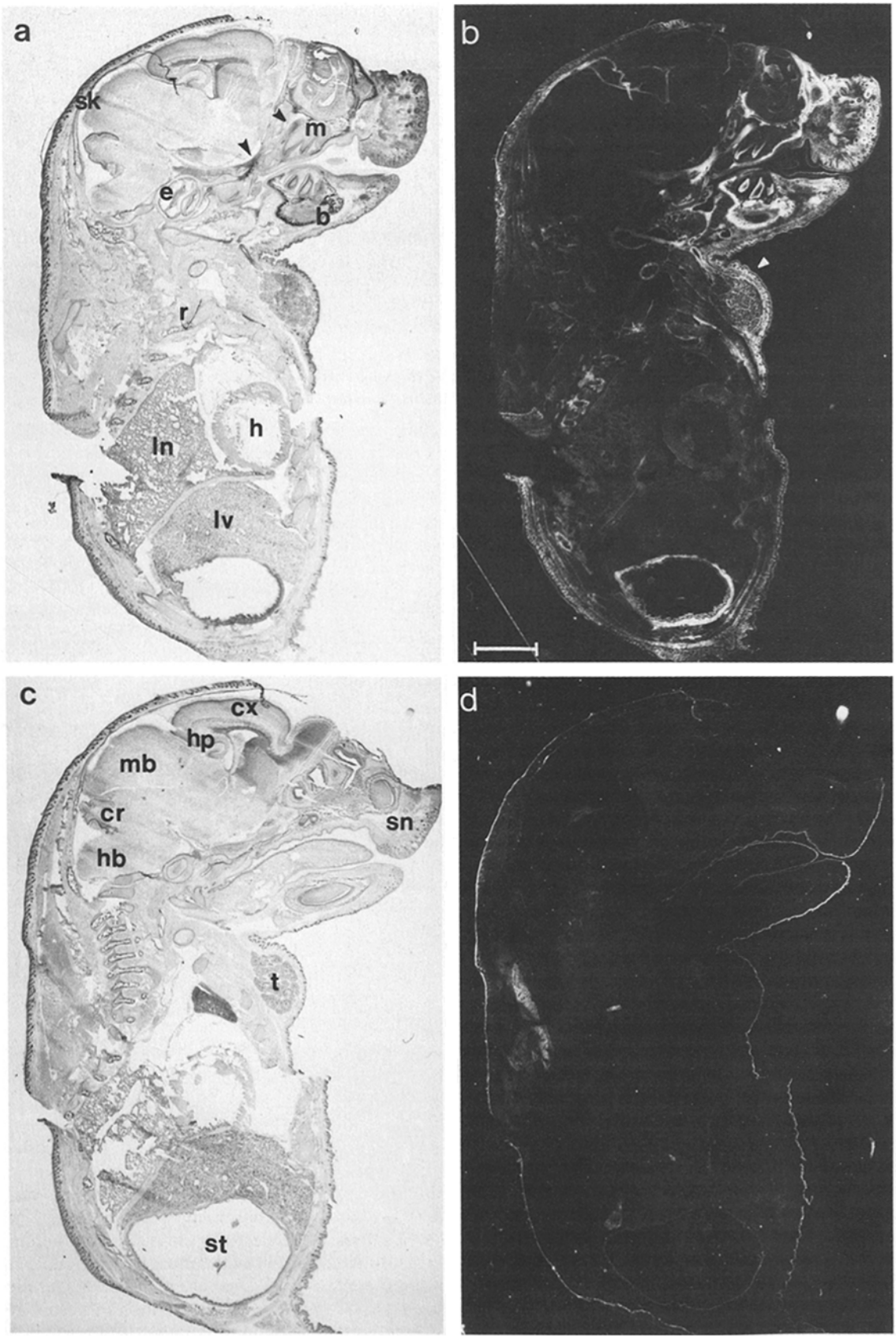

Figure 6. SPARC RNA distribution in the newborn mouse. Autoradiographs of parasagittal sections of a newborn mouse, processed for in situ hybridization with − strand probe (*a* and *b*), and + strand probe (*c* and *d*). *a* and *c* show bright field illumination, *b* and *d* show dark ground illumination. In *d* note the nonspecific concentration of silver grains on the outer surface of the epidermis. The arrow in *b* shows regions of skin detailed in Fig. 9 *b*. The arrows in *a* show infraorbital nerve trunk (see Fig. 8, *a* and *b*). The slides were exposed to emulsion for 5 d. *b*, Alveolar bone of mandible; *cr*, cerebellum; *cx*, cortex; *e*, ear; *h*, heart; *hb*, hindbrain; *hp*, hippocampus; *ln*, lung; *lv*, liver; *m*, first molar in maxilla; *mb*, midbrain; *r*, rib; *st*, stomach; *sk*, membrane bone of skull; *sn*, snout region; *t*, thyroid. Bar, 2 mm.

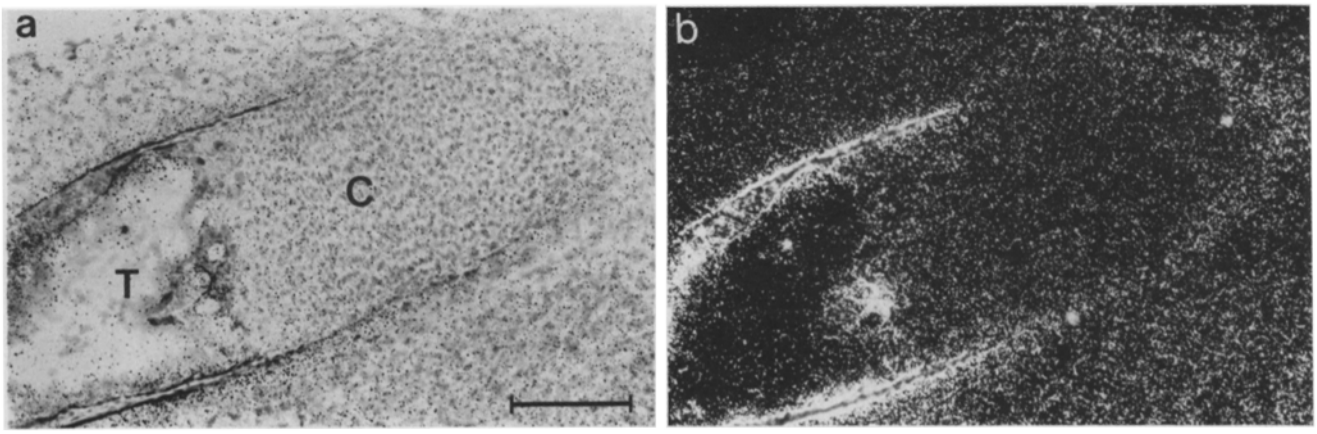

Figure 7. SPARC RNA distribution in endochondrial bone (rib) of the newborn mouse. (*a*) Autoradiograph of a tangential section of a rib processed for in situ hybridization with − strand probe, showing the region of ossification on the left and diaphysial cartilage on the right. Bright field illumination. *T*, Trabula of bone; *C*, cartilage. (*b*) Same field as in *a* photographed under dark ground illumination. Slide was exposed to emulsion for 5 d. Bar, 150 μm.

cells, which had been released from follicles immediately before ovulation and then cultured in vitro for 3 d (Fig. 4).

Testis. Expression of SPARC RNA in the testis of adult and immature 2-wk-old mice is characterized by low levels in the seminiferous tubules (containing Sertoli cells and developing spermatogonia) and high levels in the interstitial cells and capsule (Fig. 5). Again, it is not possible to distinguish between individual components of the interstitial layer, but the results are compatible with hybridization to the major cell types, including the steroid-producing Leydig cells and endothelial cells.

Distribution of SPARC RNA in the Newborn Mouse

To study SPARC expression in a wider range of tissues, sections of newborn mice were hybridized with − and + strand probes. Grain densities over some tissues (e.g., liver and most neuronal cells of the brain) were approximately equal for both probes, and these are therefore considered negative for SPARC expression (Table I). Slightly higher grain densities were seen after − strand hybridization in lung and heart, suggesting a low level of SPARC RNA in these tissues. In striking contrast, very high grain densities are associated with bones and teeth, whisker follicles, infraorbital nerve trunk, thyroid (interstitial stroma), and stomach (submucosa) (Fig. 6).

Bone. SPARC mRNA is present at high levels in bones of both the axial skeleton (sites of endochondrial ossification), and the skull and jaw (sites of membranous ossification). In the axial skeleton hybridization is strongest in cells on the periosteal and endosteal surfaces, while cartilage that has not yet been replaced by bone does not hybridize significantly above the background levels seen in the surrounding connective tissue (Fig. 7). In the alveolar bone of the jaw, hybridization is stronger on the surface away from the teeth, where bone deposition is most active, than on the inner surface of the tooth cavity, where bone resorption predominates (Fig. 8, *a* and *b*). Grain distribution is very low over small, mononucleated cells embedded within the bone matrix (Fig. 8 *d*). Since the alveolar bone is membranous, and not derived by replacement of a cartilaginous template, these internal cells are probably mature osteocytes.

Teeth. In the newborn mouse, SPARC RNA is abundant in the cytoplasm of the odontoblasts of the first molar, but is not yet expressed in the second and third molars. In the first molar, the ameloblasts, which are responsible for producing the calcified enamel, show only low levels (Fig. 8, *a*, *b*, and *c*).

Skin and Whisker Follicles. The snout region of the newborn mouse shows intense hybridization of − strand probe to the connective tissue sheath around the whisker follicles, a region rich in blood sinuses and nerve endings (Green, 1966) (Fig. 9, *a*, *c*, and *d*). SPARC RNA is also localized in the dermis of the skin in other regions of the body (Fig. 9 *b*). Silver grains over the epidermis are confined to the outermost, terminally keratinized cells, but are seen with both + and − strand probes.

Brain and Peripheral Nerve. In general, SPARC RNA is absent from neuronal cells of the newborn brain. However, localized bands of specific hybridization can be seen, for example, in the hippocampus (Fig. 6). In this region hybridization grains are abundant over the pia mater of the lateral ventricle and over cells that probably correspond to the superficial glial of the fimbria, and to the alveus. However, more detailed investigation is required before these regions can be identified unambiguously.

Sections of the head region also reveal high grain densities associated with peripheral nerve bundles, in particular the prominent infraorbital trunk, which contains the nerves running from the whiskers (Fig. 6 and Fig. 8, *a* and *b*).

Discussion

In this paper we have shown that in situ hybridization can be a powerful technique for revealing unexpectedly complex patterns of expression of a cloned gene in embryonic, neonatal, and adult mouse tissues. In this particular case the results throw new light on the biological role of osteonectin by clearly showing that expression of the gene is not confined to mineralized tissues such as bone and teeth, but is also found in a variety of other specialized cell types, often at a high level. These results are summarized in Table I. Although precise quantitation of RNA levels is difficult by in

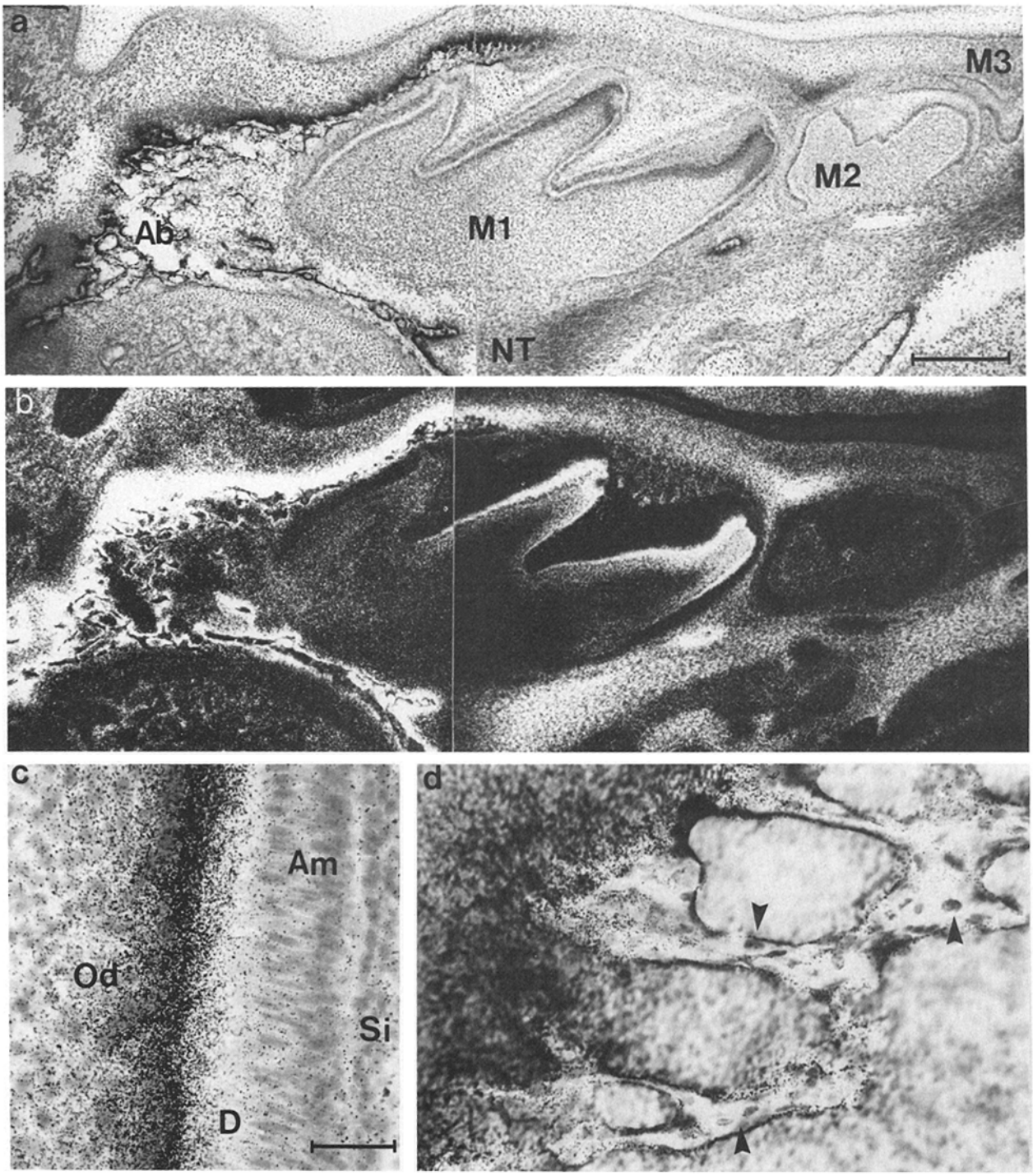

Figure 8. SPARC RNA distribution in membrane bone, teeth, and peripheral nerve trunk of newborn mouse. Autoradiograph of the maxillary region shown in Fig. 6 processed for in situ hybridization with − strand probe. Photographed under bright field (*a*) and dark ground (*b*) illumination. *Ab*, Alveolar bone; *MI–3*, first to third molars; *NT*, infraorbital nerve trunk. (*c*) Detail of first molar showing high density of silver grains over the cytoplasm of the odontoblasts (*Od*). *Am*, Ameloblast layer; *D*, dentine; *Si*, stratum intermedium. (*d*) Detail of alveolar bone. High grain density is seen in the periosteal region to the left, while small, mononucleated mature osteocytes within the bone are associated with few grains (*arrows*). Bars: (*a* and *b*) 300 μm; (*c* and *d*) 40 μm.

situ hybridization, some information can be obtained by combining the distribution data with results from Northern analysis of total extracted RNA. For example, the level of SPARC RNA in the adult adrenal gland is ~38% of that in parietal endoderm cells, where it constitutes 0.5% of total poly(A)$^+$ RNA (Mason et al., 1986*b*). Fig. 2 shows that SPARC RNA is produced almost entirely by the zona fasciculata, which makes up ~63% of the total volume of the adrenal gland. Combining these values, and assuming equal cell density throughout the adrenal, it appears that the zona

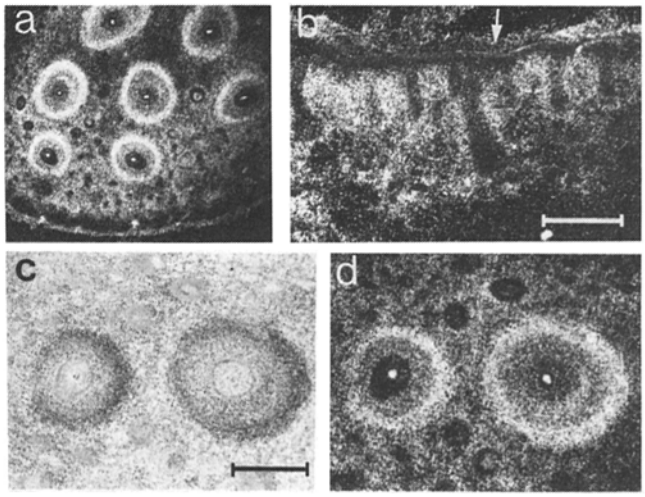

Figure 9. SPARC RNA distribution in the newborn skin. (*a*) Autoradiograph of section of the snout region from Fig. 6 showing high grain density around the whisker follicles. Dark ground illumination. (*b*) Detail of section through body skin from Fig. 6 showing high grain density in the dermis. Dark ground illumination. The concentration of silver grains over the outer layer of the epidermis (*E*) is also seen in sections processed with + strand probes (see Fig. 6). (*c* and *d*) Detail of *a* at higher magnification. Bright field (*c*) and dark ground illumination (*d*). Slides were exposed to emulsion for 5 d. Bars: (*a* and *b*) 450 μm; (*c* and *d*) 150 μm.

fasciculata cells contain ~60% the amount of SPARC RNA as parietal endoderm cells. Thus, data on the spatial distribution of RNA can be used to expand and complement quantitative Northern data (Mason et al., 1986*a*, *b*; Young et al., 1986). Consideration must also be given to the fact that RNA levels do not necessarily reflect protein levels in a given tissue. For example, Sage and co-workers, using affinity-purified polyclonal antibodies to SPARC on mouse tissues, have observed differences in SPARC mRNA and protein levels in some tissues (H. Sage, University of Washington, Seattle, WA, personal communication).

The results obtained here suggest that the role of SPARC/osteonectin encompasses more than just promoting matrix mineralization. In particular, high levels of SPARC expression appear to be correlated with at least two other important biological processes; synthesis and assembly of basement membrane components (e.g., laminin and type IV collagen) and steroid production. Examples in the first category are parietal endoderm (Hogan et al., 1984), endometrial cells of the deciduum (Wewer et al., 1986), Schwann cells of the peripheral nerve (Bunge et al., 1986; Dziadek et al., 1987), endothelial cells adjacent to the glomerular basement membrane (data not shown), dermal fibroblasts in newborn skin (Hogan et al., 1982), and aortic endothelial cells in culture (Sage et al., 1984). Evidence for an apparent correlation between steroid production and SPARC expression comes from the high level of RNA and/or protein synthesis seen in the zona fasciculata of the adrenal (Fig. 2), thecal, and granulosa cells of the ovary (Figs. 3 and 4), and interstitial cells of the testis (Fig. 5), as well as Leydig cells isolated from rat testis (Hogan, B. L. M., and B. Cooke, unpublished observations).

Given that a reassessment of osteonectin function is required, what alternative role is compatible with the pattern of gene expression revealed by this study? At present we can only speculate. One possibility, based on the observation that osteonectin at low concentrations delays hydroxyapatite-seeded crystal growth (Romberg et al., 1985), is that the protein plays a role in preventing, rather than promoting, matrix mineralization. This may be important, for example, during the early stages of fetal bone morphogenesis when the type I collagen matrix is first being laid down. As the osteocytes mature, local levels of SPARC may decline as a result of lower levels of gene expression (see Fig. 8 *d*), gradually allowing crystal growth to proceed in an orderly way. This hypothesis requires that local extracellular concentrations of SPARC in the tissues exceed the value of ~5 μg/ml (1.6×10^{-7} M) which was found by Romberg et al. (1985) to inhibit by 50% hydroxyapatite-seeded crystal growth in a saturated calcium phosphate solution. Although few quantitative measurements of SPARC/osteonectin/BM40 concentrations in tissues are at present available, it represents 2–3% of the total protein in fetal bovine bone matrix (Termine et al., 1981*a*), and a value of 244 μg/g wet weight has been reported for the protein BM-40 in the EHS tumor (Dziadek et al., 1986). Local regulation of free Ca^{++} levels may also play a role in the ordered assembly of basement membrane components, since there is evidence that association of laminin molecules into a three-dimensional matrix requires Ca^{++} (Yurchenco et al., 1985). Finally, stimulation of steroid production appears to be associated with a transient increase in intracellular Ca^{++} (for example, Sullivan and Cooke, 1986). This raises the possibility that high levels of steroidogenesis may involve fluxes of Ca^{++} into and out of cells, and a risk of Ca^{++} deposition in the surrounding matrix, which may be reduced by the local secretion of SPARC. This predicts that SPARC expression may be modulated by the level of steroidogenic activity of a tissue, a testable hypothesis.

In conclusion, the technique of in situ hybridization described here opens up the possibility of following changes in SPARC expression in specific cells within an organ after treatments designed to change physiological activity in vivo. Experiments are also in progress to follow the temporal and spatial pattern of SPARC gene expression during complex morphogenetic processes such as bone development and angiogenesis.

We thank many friends and colleagues for helpful suggestions in the course of this work, in particular Drs. Andrew Lumsden, Dennis Summerbell, Robb Krumlauf, Shintaro Nomura, Helene Sage, Mats Paulsson, and Geoffrey Raisman. We are also grateful to Mrs. Lydia Pearson for patiently preparing the manuscript, Neal Papworth for photography, Jennifer Hanson for performing the immunoprecipitation experiment, and Dr. Colin Hetherington for animal services.

Received for publication 13 February 1987, and in revised form 24 March 1987.

References

Brûlet, P., H. Condamine, and F. Jacob. 1985. Spatial distribution of transcripts of the long repeated ET_n sequence during early mouse embryogenesis. *Proc. Natl. Acad. Sci. USA.* 82:2054–2058.

Bunge, R. P., M. B. Bunge, and C. F. Eldridge. 1986. Linkage between axonal ensheathment and basal lamina production by Schwann cells. *Annu. Rev. Neurosci.* 9:305–328.

Cox, K. H., D. V. DeLeon, L. M. Angerer, and R. C. Angerer. 1984. Detection of mRNAs in sea urchin embryos by *in situ* hybridization using asym-

metric RNA probes. *Dev. Biol.* 101:485–502.
Dang, C. V., R. F. Ebert, and W. R. Bell. 1985. Localization of a fibrinogen calcium binding site between γ-subunit positions 311 and 336 by terbium fluorescence. *J. Biol. Chem.* 260:9713–9719.
Dziadek, M., M. Paulsson, M. Aumailley, and R. Timpl. 1986. Purification and tissue distribution of a small protein (BM40) extracted from a basement membrane tumor. *Eur. J. Biochem.* 161:455–464.
Green, E.L., editor. 1966. Biology of the Laboratory Mouse. 2nd ed. McGraw-Hill, New York. 266.
Hafen, E., M. Levine, R. L. Garber, and W. J. Gehring. 1983. An improved *in situ* hybridization method for the detection of cellular RNAs in *Drosophila* tissue sections and its application for localizing transcripts of the homeotic *Antennapedia* gene complex. *EMBO (Eur. Mol. Biol. Organ.) J.* 2:617–623.
Hogan, B. L. M., D. P. Barlow, and M. Kurkinen. 1984. Reichert's membrane as a model for studying the biosynthesis and assembly of basement membrane components. *CIBA Found. Symp.* 108:60–69.
Hogan, B., F. Costantini, and E. Lacy. 1986. Manipulating the Mouse Embryo: A Laboratory Manual. Cold Spring Harbor Laboratory, Cold Spring Harbor, New York. pp. 131 and 236.
Hogan, B. L. M., A. Taylor, M. Kurkinen, and J.R. Couchman. 1982. Synthesis and localization of two sulphated glycoproteins associated with basement membranes and the extracellular matrix. *J. Cell Biol.* 95:197–204.
Ingham, P. W., K. R. Howard, and D. Ish-Horowicz. 1985. Transcription pattern of the *Drosophila* segmentation gene *hairy. Nature (Lond.).* 318:439–445.
Kretsinger, R. H. 1979. The informational role of calcium in the cytosol. *Adv. Cyclic Nucleotide Res.* 11:1–26.
Maniatis, T., E. F. Fritsch, and J. Sambrook. 1982. Molecular Cloning: A Laboratory Manual. Cold Spring Harbor Laboratory, Cold Spring Harbor, New York. pp. 202–203.
Mason, I.J., A. Taylor, J. G. Williams, H. Sage, and B. L. M. Hogan. 1986*a*. Evidence from molecular cloning that SPARC, a major product of mouse embryo parietal endoderm, is related to an endothelial cell 'culture shock' glycoprotein of M_r 43,000. *EMBO (Eur. Mol. Biol. Organ.) J.* 5:1465–1472.
Mason, I. J., D. Murphy, M. Munke, U. Francke, R. W. Elliott, and B. L. M. Hogan. 1986*b*. Developmental and transformation-sensitive expression of the *Sparc* gene on mouse chromosome 11. *EMBO (Eur. Mol. Biol. Organ.) J.* 5:1831–1837.
Melton, D. A., P. A. Krieg, M. R. Rebagliati, T. Maniatis, K. Zinn, and M. R. Green. 1984. Efficient *in vitro* synthesis of biologically active RNA and RNA hybridization probes from plasmids containing a bacteriophage SP6 promoter. *Nucleic Acids Res.* 12:7035–7056.
Rogers, A. W. 1979. Techniques of Autoradiography. 3rd ed. Elsevier, North Holland. pp. 368–370.
Romberg, R. W., P. G. Werness, P. Lollar, B. Lawrence Riggs, and K. G. Mann. 1985. Isolation and characterization of native adult osteonectin. *J. Biol. Chem.* 260:2728–2736.
Sage, H. 1985. Low molecular weight fibroblast collagen: structure, secretion, and differential expression as a function of fetal and cellular age. *Biochemistry.* 24:7430–7440.
Sage, H. 1986. Culture shock. Selective uptake and rapid release of a novel serum protein by endothelial cells *in vitro. J. Biol. Chem.* 261:7082–7092.
Sage, H., C. Johnson, and P. Bornstein. 1984. Characterization of a novel serum albumin-binding glycoprotein secreted by endothelial cells in culture. *J. Biol. Chem.* 259:3993–4007.
Sullivan, M. H. F., and B. A. Cooke. 1986. The role of Ca^{++} in steroidogenesis in Leydig cells. *Biochem. J.* 236:45–51.
Szebenyi, D. M. E., and K. Moffat. 1986. The refined structure of vitamin D-dependent calcium-binding protein from bovine intestine. *J. Biol. Chem.* 261:8761–8777.
Termine, J. D., A. B. Belcourt, K. M. Conn, and H. K. Kleinman. 1981*a*. Mineral and collagen-binding proteins of fetal calf bone. *J. Biol. Chem.* 256:10403–10408.
Termine, J. D., H. K. Kleinman, S. W. Whitson, K. M. Conn, M. L. McGarvey, and G. R Martin. 1981*b*. Osteonectin, a bone-specific protein linking mineral to collagen. *Cell.* 26:99–105.
Tung, P. S., C. Domenicucci, S. Wasi, and J. Sodek. 1985. Specific immunohistochemical localisation of osteonectin and collagen types I and III in fetal and adult porcine dental tissues. *J. Histochem. Cytochem.* 33:531–540.
Wasi, S., K. Otsuka, K.-L. Yao, P. S. Tung, J. E. Aubin, and J. Sodek. 1984. An osteonectin-like protein in porcine periodontal ligament and its synthesis by periodontal ligament fibroblasts. *Can. J. Biochem. Cell Biol.* 62:470–477.
Wewer, U. M., A. Damjanov, J. Weiss, L. A. Liotta, and I. Damjanov. 1986. Mouse endometrial stromal cells produce basement-membrane components. *Differentiation.* 32:49–58.
Young, M. F., M. E. Bolander, A. A. Day, C. I. Ramis, P. G. Robey, Y. Yamada, and J. D. Termine. 1986. Osteonectin mRNA: distribution in normal and transformed cells. *Nucl. Acids Res.* 14:4483–4497.
Yurchenco, P. D., E. C. Tsilibary, A. S. Charonis, and H. Furthmayr. 1985. Laminin polymerisation *in vitro.* Evidence for a two-step assembly with domain specificity. *J. Biol. Chem.* 260:7636–7644.